

Behavior of reinforced sustainable concrete hollow-core slabs

Adel A. Al-Azzawi* and Mustafa S. Shallal^a

Department of Civil Engineering, Al-Nahrain University, Baghdad, Iraq

(Received December 29, 2018, Revised January 26, 2021, Accepted February 10, 2021)

Abstract. This study aims to trace the response of twelve one-way sustainable concrete hollow-core slabs made by reducing cement content and using replacement of coarse aggregate by plastic aggregate. The trial mixes comprise the 25, 50, 75, and 100% replacement of natural coarse aggregate. The compressive strength of the resulting lightweight concrete with full replacement of coarse aggregate by plastic aggregate was 28 MPa. These slabs are considered to have a reduced dead weight due to using lightweight aggregate and due to reducing cross-section through using voids. The samples are tested under two verticals line loads. Several parameters are varied in this study such as; nature of coarse aggregate (natural or recycled), slab line load location, the shape of the core, core diameter, flexural reinforcement ratio, and thickness of the slab. Strain gauges are used in the present study to measure the strain of steel in each slab. The test samples were fourteen one-way reinforced concrete slabs. The slab's dimensions are (1000 mm), (600 mm), (200 mm), (length, width, and thickness). The change in the shape of the core from circular to square and the use of (100 mm) side length led to reducing the weight by about (46%). The cracking and ultimate strength is reduced by about (5%-6%) respectively. With similar values of deflection. The mode of failure will remain flexural. It is recognized that when the thickness of the slab changed from (200 mm to 175 mm) the result shows a reduction in cracking and ultimate strength by about (6% and 7%) respectively.

Keywords: hollow core slabs; recycled aggregate; PVC plastic aggregate; reinforced concrete; experimental tests; steel reinforcement

1. Introduction

Natural aggregate concrete is widely used in cast structural members (Daud 2015, Daud 2018). Nowadays, recycled aggregate incorporation in concrete is a recent development in the use of various types of waste materials in concrete production (de Brito and Saikia 2013, Al-Azzawi and Al-Azzawi 2020, Al-Azzawi *et al.* 2020). The rigid Polyvinyl chloride (PVC) has been used effectively in different applications and generates huge waste material. It is important to dispose of this waste material by reusing it in the concrete composition. This application may save energy and reduce the demand for primary mineral resources. Therefore the reuse of plastic waste material in concrete is considered the best environmental alternative method to reduce environmental pollution and safeguarding natural resources (Alamgir and Ahsan 2007). Hollow-core slab HCS is defined as slab-made precast, pre-stressed one with longitudinal voids developed in the length of the slab to decrease weight and cost. The voids may be used to insert electrical or mechanical runs.

A longer span length of HCS is used and reaches up to (18 m) without inserting supporting members. Precast pre-stressed HCS is used in bridges and longer span slabs under heavy loads. Precast pre-stressed HCS are members with maximum structural efficiency when high-strength concrete

is used. The HCS slab requires lesser material consumption (Stephen 2013).

Abramski *et al.* (2010) analyzed and studied the shear capacity of two-way hollow core slabs (HCS). Thirteen full-scale specimens and identical nonlinear finite element (FE) computations were made to show that the strength of shear of a two-way HCS is at fifty percent of the strength of shear of the solid slab. The stiffness of a two-way HCS should be determined like they are specified for a solid slab. The specimen and the nonlinear FE computations for this study have demonstrated that it is correct to calculate the internal forces of a two-way HCS in the same way like they are determined for a solid slab.

Rahman *et al.* (2012) prestressed precast hollow core slabs (PPHCS) were used. The design of those construction units is founded on the ultimate load-carrying capacity of those members. Full-scale load tests were demonstrated on PPHCS with varying (a/d) ratio, which was loaded to achieve the ultimate capacity of those slabs. A total of fifteen samples have 500 and 250 cm in span and 3 varying depths, 20, 25, and 30 cm were tested using a 4-point load test. The slabs were reinforced with conventional prestressing strands. And the number of prestressing strands was increased with the depth of the slab. It was noted that the failure mode of the slabs was changed from pure flexure to flexure-shear mode for slabs with a depth bigger than 20 cm. If the slab thickness is enlarged, the web shear cracking strength of PPHCS is decreased. A transition from flexure-shear to shear failure as a function of a/d was observed. The analysis of the experimental outcomes displayed that the existing ACI code equations underestimated the flexure-

*Corresponding author, Professor
E-mail: dr_adel_azzawi@yahoo.com
^aM.Sc.

shear strength of those HCS. Based on regression analysis of experimental data, a modification is suggested in the present ACI code equation which captured exactly the ultimate load-carrying capacity and the mode of failure of those slabs.

Said *et al.* (2012) suggested a strut-and-tie model forecast the failure mode, ultimate load-carrying capacity, and design of prestressed precast hollow core slabs (PPHCS). In that suggested model for PPHCS without shear reinforcement, the tension forces were opposed by prestressing tendons (tension tie), the compression forces were withstood by concrete compression struts, and the tensile forces in the web were opposite by concrete tension elements (concrete ties). The outcomes gained from the suggested STM model by utilizing the software of computer-aided strut and tie (CAST) are compared with those gained from full-scale loading tests on fifteen PPHCS of the various (a/d). The suggested strut-and-tie model showed a good correlation with the experimental outcomes and the procedure could be without problem utilized for analysis and design of HCS.

Brunesi, *et al.* (2014) carried out a comparison between experimental, analytical, and finite element method for shear strength capacity of precast pre-stressed concrete hollow core slabs with (200-500) mm thick without transverse reinforcement through a nonlinear finite element analysis, which matched the experiments test data. These members (49 specimens) are characterized with six nominal slab depths, five hollow shapes with circular and non-circular voids, different voids ratios, several pre-stressing steel strands arrangements, and levels of initial pre-stress then comparative with traditional codes. From finite element (FE) results, the proposed numerical approach was validated by focusing on a single precast prestressed hollow-core unit, therefore the accuracy of the FE predictions obtained for nine specimens analyzed was quantified in comparison with experimental data.

Haruna (2014) studied the flexural behavior of precast pre-stressed concrete hollow-core units with cast-in-place concrete topping, through load testing of five full-scale specimens. The specimens were divided into two groups wide and narrow. The presence of a cast-in-place topping slab improved the behavior of hollow-core units by increasing the flexural crack initiation and maximum load capacities as well as the stiffness. As a result of premature loss of composite behavior, the predicted load capacity of these specimens assuming a fully composite behavior remained on the non-conservative side. The obtained results suggested that the floor system made of cast-in-place concrete topping placed over the machine-finished surface of precast concrete hollow-core units with no interfacial roughening is not able to provide the interface shear strength required to develop a fully composite behavior.

Lee *et al.* (2014) studied the web shear capacity of hollow core slabs (HCS) through a large number of shear tests. The analysis of results indicated that the minimum shear reinforcement requirement for deep HCS members is too severe and that the web-shear strength equation in ACI 318 code does not provide a good estimation of shear strengths for HCS members. Thus, a rational web-shear

strength equation for HCS members was derived in a simple manner, which provides a consistent margin of safety on shear strength for the HCS members up to 500 mm deep. More shear test data would be required to apply the proposed shear strength equation for the HCS members over 500 mm in depth though.

Yang *et al.* (2014) studied the effects of using varying amounts of carbon fiber reinforced plastics (CFRP) strengthening prestressed concrete hollow core slabs (PPHCS) and the capacity study procedures. Test data of sixth slabs reinforced with CFRP with various amounts were compared to gain an available formula of flexural capacity. The outcomes demonstrated that the bearing capacity and ductility of those slabs were significantly enhanced with adding of CFRP. The suggested procedure of calculation was simple, safe, practical, and high accuracy, the calculation outcomes correspond well with experimental outcomes, and it had a certain reference value for the calculation of the followed studies and practical projects.

Al-Azzawi and Abed (2017) presented an investigation on the behavior of moderately thick hollow core slabs (HCS) with various parameters. Part of this research includes cast and test 8-slabs of solid and hollow-core slab having (2000 mm), (600 mm), and (250 mm) (length, width, thickness). Load deflection curve was noted. And the other part (numerical part), the (FE) procedure was utilized to show the behavior of those slabs by employed ANSYS program. The FE analysis displayed good agreement as compared with the experimental results with a difference of about (5%-8.70%) in ultimate loads. A parametric study was conducted by utilizing the ANSYS program to discuss the effects of the concrete shape of the core, compressive strength, and size, type of applied load, and effect of removing top steel reinforcement.

Al-Azzawi and Al-Asdi (2017) tested eleven slab specimens which are made one way though using two simple supports. The tested specimens comprised three reference solid slabs and eight styropor block slabs having (23 % and 29%) weight reduction. The voids in slabs were made using styropor at the ineffective concrete zones in resisting the tensile stresses. All slab specimens have the dimensions (1100×600×120 mm) except one solid specimen has a depth 85 mm (to give a reduction in weight of 29% which is equal to the styropor block slab reduction). Two loading positions or cases (A and B) (as two-line monotonic loads) with shear span to effective depth ratio of ($a/d=3, 2$) respectively, were used to trace the structural behavior of styropor block slab. The best results are obtained for styropor block slab strengthened by minimum shear reinforcement with a weight reduction of (29%).

Wariyatno *et al.* (2017) tested samples consist of a solid slab as a reference and a hollow core slab (HCS) type 1 (use PVC pipes to create cavities) and an HCS type 2 (utilizing Styrofoam to create the cavities). The slab thickness was 120 mm; the result revealed that HCS type 1 and 2 can reduce weight by (24.0%) and (25.0%) as compared to the reference. The flexural strength of HCS type 2 was higher than the (HCS) type 1, however, it was lower than the solid slab with all variations in reinforcement diameter. The value of the flexural stiffness of the solid slab was greater than

HCS types 1 and 2. Cracks that occur in the solid slab are distinguished as flexural cracks, while the cracks that occur in the HCS type 1 and 2 are shear cracks.

Al-Azzawi and Abdul Al-Aziz (2018) investigated the behavior of reinforced normal and lightweight aggregate concrete hollow core slabs with different core shapes, shear span to effective depth (a/d). The experimental work includes testing seven reinforced concrete slabs under two vertical line loads. The dimensions of slab specimens were (1.1 m) length, (0.6 m) width, and (0.12 m) thickness. The maximum reduction in weight due to aggregate type was (19.28%) and due to cross-section (square and circular) cores were (17.37 and 13.64%) respectively. The test results showed that the decrease of shear span to effective depth ratio from 2.9 to 1.9 for lightweight aggregate solid slab cause an increase in ultimate load by (29.06%) and increase in the deflection value at ultimate load or the ultimate deflection by (17.79%).

The use of plastic waste in the structural members are made through the following researchers.

The actions of PET-containing reinforced concrete beams was studied by Mohammed (2017). Particles of PET have been shredded and the fine aggregate replaced with 5, 10, and 15%. The beams have been slightly strengthened with a steel shaft and have been designed to fail. PET waste caused a 12 to 21 percent reduction in compressive power. Recycled PET waste reinforced cement is almost equivalent to regular beams for stiffness and failure. The ultimate capacity is small decreased and the load-deflection response slightly changes when up to 15% of the PET waste is used. PET was also used as fiber by Khalid *et al.* (2018) in another investigation on reinforced concrete beams. In the concrete mixtures, four separate PET types were used; ring-formed, irregularly shaped, plastic waste wire, and synthetic macro-fiber made. A total of 18 beams were cast and their flexural actions were measured by four stages. The tests indicated that it did not minimize deflection by applying Pet ringed fibers to reinforced concrete beams. With ring-shaped PET fibers, the ductility for reinforced concrete beams was increased in comparison to other fiber types.

Khatib, *et al.* (2019) investigated the response of reinforced concrete beams containing waste plastic. The plastic was the cap of a bottle of plastic. It has prepared four concrete mixes. The field aggregate has been replaced by 0, 10%, 15%, and 20% waste plastic (by volume). The water-to-cement ratio of all mixtures was stable. At 20°C for 28 days, all beams were cured. By analyzing the central deflection of the beam at different load intervals before failure, the structural performance was assessed. The failure mode was also visually examined. The findings suggested that a certain amount of waste plastic can be used without compromising the flexural properties of reinforced concrete beams in structural applications.

Based on previous studies, there has been limited research on the structural assessment of reinforced concrete structural members containing waste plastic especially slabs. Also, the reduction in weight due to both material and cross-section using recycled material with sustainable concrete has not yet been investigated. In the present research, two types of reduction in weight are achieved through using recycled PVC as lightweight aggregate

Table 1 Grading of recycled coarse aggregate

Sieve size (mm)	Passing %	Limit of Iraqi Specification No. 45 (1984)
12.5	100	100
9.5	94.24	85-100
4.75	60.42	10-30
2.36	2.3	0-10

(LWA) and hollow cores (HC). And therefore, the main objective of this study is to produce and investigate the behavior of lighter one way reinforced sustainable concrete slab with reduced weight experimentally.

2. Experimental program

2.1 Materials and mix

The chemical and physical tests result of the used Type I cement is conformed to the Iraqi Specification No. 5/1984.

2.1.1 Fine aggregate

The fine aggregate (sand) has (4.75 mm) maximum size with a smooth texture and rounded particle shape with fineness modulus of (2.84). The sand sieve analysis is relevant to the Iraqi Specification No. 45/1984.

2.1.2 Natural coarse aggregate

The maximum size of (10 mm) crushed gravel was used in the concrete blends. The specific gravity was (2.64). The coarse aggregate sieve analysis is relevant to the Iraqi Specification No. 45/1984.

2.1.3 Recycled coarse aggregate

PVC plastic waste collected from the manufacturing of doors and windows wastes is used as coarse recycled aggregates with the maximum nominal size of 10 mm in this study. The specific gravity was (1.36). The grading of recycled coarse aggregate is shown in Table 1. The characteristics of the aggregates were established in order to study their possible application in concrete production.

2.1.4 Super plasticizer

The superplasticizer used in this work was PCE 600 which has been primarily developed for applications in the precast, lightweight, and aerated concrete industries. PCE 600 is different than conventional superplasticizer based on sulfonated melamine and naphthalene formaldehyde condensate, which create electrostatic repulsion of particles. The superplasticizer is used throughout this work as a percentage by weight of cement.

2.1.5 Mineral admixture (Silica Fume (SF))

The silica fume used in this work complies with the physical and chemical requirements of ASTM C1240. A grey silica fume brought from Sika Company for chemicals has been used in the present study.

2.1.6 Concrete mixtures

Table 2 Mix proportion of natural and plastic aggregate concrete mixtures

Mix type	Natural aggregate	Plastic aggregate 100% replacement
Cement content (kg/m ³)	275	400
Sand (kg/m ³)	800	625
Gravel or natural aggregate (kg/m ³)	1000	0
Plastic or PVC aggregate (kg/m ³)	0	945
Superplasticizer by weight of cement (%)	2	2
Silica Fume replacement of cement	15	15
Water cement ratio	0.36	0.34

Sixteen mixtures have been designed with different proportions to study the effect of PVC recycled aggregate on the mechanical properties of concrete and too to prepare sustainable concrete. The required compressive strength of this study was (28 MPa) for both natural coarse aggregate concrete (NAC) and (RAC) recycled coarse aggregate concrete. The ACI mix design method ACI 211.1/1991 is used to design the concrete mixtures. The blends are shown in Table 2.

For the slab specimens, the properties of the hardened concrete for the average of three samples and steel reinforcement used for casting these slabs are summarized in Table 3.

2.2 Slab specimen's details and testing procedure

The test samples comprise twelve one-way reinforced concrete slabs subjected to two vertical line loads. The slab's dimensions are (1000 mm), (600 mm), (200 mm), (length, width, and thickness) respectively except slab 12 which has a thickness (175), and slab1 which has the same slab dimensions as Al-Azzawi and Abdul Al-Aziz (2018) (1100) length, (600 mm) width, and (120 mm) thickness which is made for comparison and verification. The main reinforcement includes 5 bars of diameter (ϕ 8 mm) (main steel reinforcement ratio $\rho=0.002$) for both top and bottom while the secondary reinforcement (transverse) includes 8 bars with (ϕ 8 mm) and has a spacing of 125 mm also for both top and bottom. The flexural reinforcement for slabs (2 to 12) is the same except slab 11 which has 8 bars of diameter (ϕ 8 mm) for top and bottom in short and directions (main steel reinforcement ratio $\rho=0.004$). The study parameters were the nature of coarse aggregate (natural or plastic), slab line load location, the shape of the core, core diameter, flexural reinforcement ratio, and thickness of the slab. Strain gauges are used in the present study to measure the strain of steel in each slab. The descriptions and abbreviations of the tested slabs and their weight reduction percentages are presented in Table 4. Fig. 1 shows the details of the cast samples. According to the table, the maximum weight reduction is obtained for slab 10 (plastic aggregate concrete hollow square core slab with a core edge length of 100 mm) which is 46% compared to the natural aggregate concrete solid slab 2. For the plastic aggregate concrete hollow circular core (core diameter 100

Table 3 Properties of materials

Properties of natural aggregate concrete		
Property	Experimental	ACI318M (2014)
Dry density (γ_c) (kg/m ³)	2408	-
Compressive strength (f'_c) (MPa)	26.9	-
Splitting tensile strength (f'_{ct}) (MPa)	3.02	2.9 (0.5 $\sqrt{f'_c}$)
Modulus of rupture (f_r) (MPa)	3.34	3.70 (0.62 $\sqrt{f'_c}$)
Modulus of elasticity (E_c) (MPa)	23950	26352 (4700 $\sqrt{f'_c}$) (W _c ^{1.5} 0.043 $\sqrt{f'_c}$)
Properties of recycled PVC aggregate concrete		
Dry density (γ_c) (kg/m ³)	1905	-
Compressive strength (f'_c) (MPa)	27.6	-
Splitting tensile strength (f'_{ct}) (MPa)	2.72	2.5 (0.8*0.5 $\sqrt{f'_c}$)
Modulus of rupture (f_r) (MPa)	2.91	2.76(0.8*0.62 $\sqrt{f'_c}$)
Modulus of elasticity (E_c) (MPa)	19622	18783 (4700 $\sqrt{f'_c}$) ($\gamma_c^{1.5}0.043\sqrt{f'_c}$)
Properties of steel reinforcement material		
Property	Test results	
Nominal diameter (mm)	8	
Calculated diameter (mm)	7.88	
Yield stress (f_y) (MPa)	377	
Ultimate stress (f_u) (MPa)	710	

mm) or slab 9, the obtained weight reduction is 41%.

The slabs were tested using (100 kN) capacity universal hydraulic testing machine available at the Structural Laboratory of Civil Engineering Department/AL-Nahrain University and using displacement control method to test all specimens. Each slab specimen was taken out from the curing container, cleaned, and painted with white paint on all sides, to observe clear visibility of cracks development during testing. The slabs have been tested at age of 28-35 days. The slab was labeled and carefully placed along the edges on simple supports. And the loads were applied at two lines at a distance of (250 and 350 mm) from support. The dial gauges were positioned at their places at the center and at the edge of the slab and the distance between the two line loading is (300 mm) for most specimens. The slabs are placed inside the machine; all apparatuses were set as shown in Fig. 2. At first, the solid steel circular supports were installed with the required center to center span length (900 mm). The load was transferred to the slabs via a

Table 4 Properties of the tested slabs with main variables

Slab No.	Type and Description	Abbreviation	Reduction in Weight (%)
1	different slab Dimensions (1100×600×120 mm) of Plastic aggregate Hollow Circular core Slab with shear span to effective depth ratio ($a/d=1.9$) and core diameter 50 mm (is made for comparison with the previous study (Verification sample).	DPHCS50-1.9	35
2	Natural aggregate Solid Slab with shear span to effective depth ratio ($a/d=2.1$)	NSS0-2.1	0.0
3	Plastic aggregate Solid Slab with shear span to effective depth ratio ($a/d=2.1$)	PSS0-2.1	21
4	Natural aggregate Hollow Circular core Slab with core diameter 75 mm and shear span to effective depth ratio ($a/d=2.1$)	NHCS75-2.1	11
5	Natural aggregate Hollow Circular core Slab with core diameter 75 mm and shear span to effective depth ratio ($a/d=1.4$)	NHCS75-1.4	11
6	Plastic aggregate Hollow Circular core Slab with core diameter 75 mm and shear span to effective depth ratio ($a/d=2.1$)	PHCS75-2.1	32
7	Plastic aggregate Hollow Circular core Slab with core diameter 75 mm and shear span to effective depth ratio ($a/d=1.4$)	PHCS75-1.4	32
8	Natural aggregate Hollow Circular core Slab with core diameter 100 mm and shear span to effective depth ratio ($a/d=2.1$)	NHCS100-2.1	20
9	Plastic aggregate Hollow Circular core Slab with core diameter 100 mm and shear span to effective depth ratio ($a/d=2.1$)	PHCS100-2.1	41
10	Plastic aggregate Hollow Square core Slab with core side length 100 mm and shear span to effective depth ratio ($a/d=2.1$)	PHSS100-2.1	46
11	different Flexural reinforcement ratio of Plastic aggregate Hollow Circular core Slab with core diameter 100 mm and shear span to effective depth ratio ($a/d=2.1$)	FPHCS100-2.1	41
12	different Thickness (175 mm) of Plastic aggregate Hollow Circular Core Slab with core diameter 75 mm and shear span to effective depth ratio ($a/d=2.1$)	TPHCS75-2.1	32

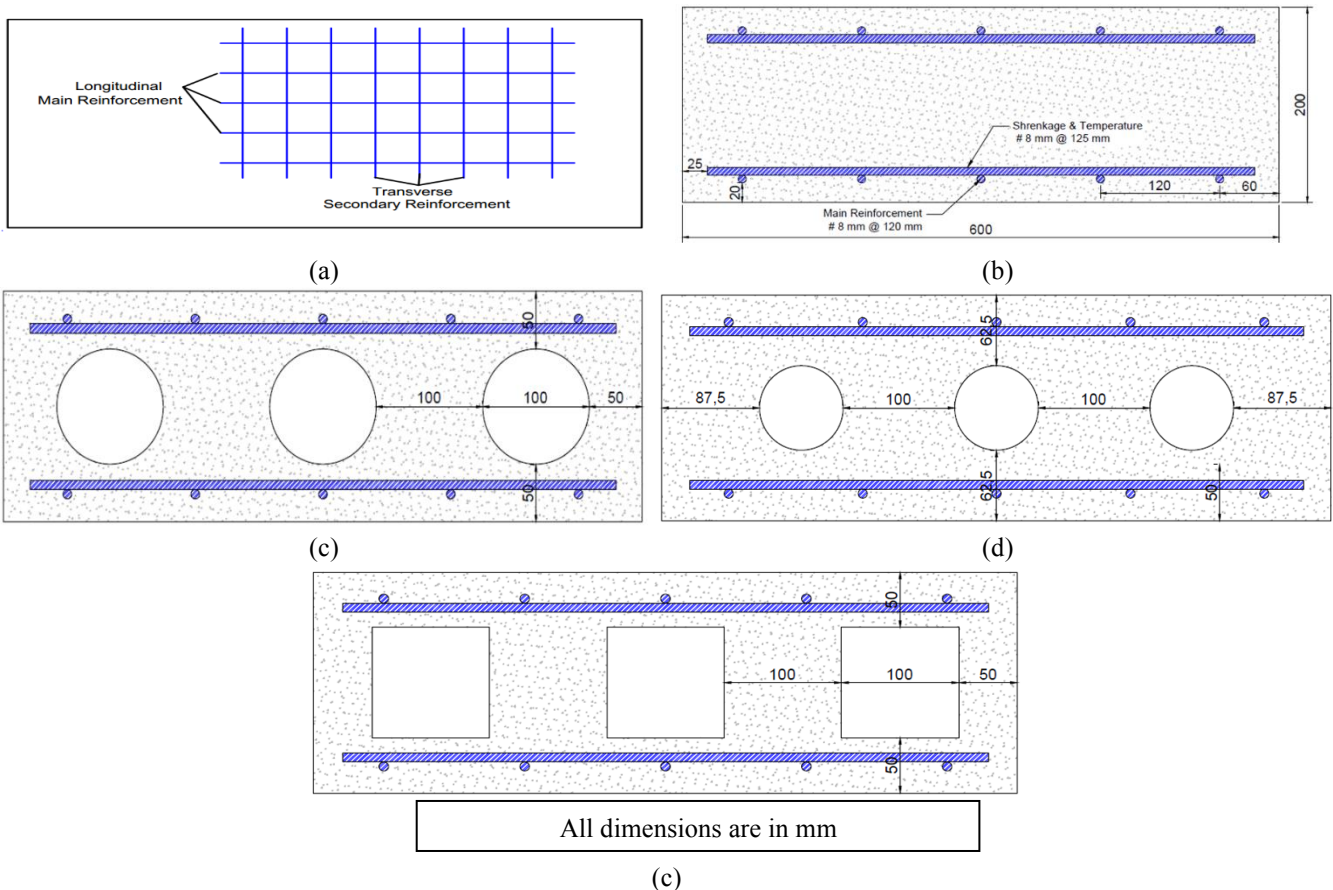


Fig. 1 (a) Specimens geometry and details (b) Solid slab (c), (d) & (e) Hollow core slabs

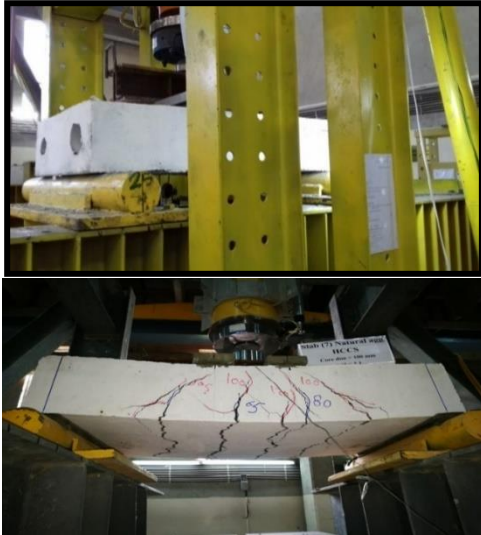


Fig. 2 Testing machine and slab sample

loading frame bridge. Steel plates (50 mm) width and (610 mm) long were put under two lines loading with rubber piece to prevent the crushing of concrete surface. After installation of the specimen over the supports, an I-section steel beam was set over the specimen with width (350 mm) and a total length of (600 mm) and was put on the central part of the tested slabs in order to distribute the applied two-line loads. The load was applied in increments of (1 kN) and at each increment of loading, the vertical deflection was measured.

3. Experimental test results

The obtained experimental results are presented and then discussed in this section. Experimental measurements which are carried out by testing fourteen slabs including the ultimate loads, load-deflection curves are given.



Slab-1 (DPHCS50-1.9)



Al-Azzawi and Abdul-Aziz (2018) tested slab

Fig. 3 Crack pattern at ultimate load for present study and previous study slabs

Comparisons between the slabs are made. Strain gauges are utilized also. The summary of experimental test results and description of samples are given in Table 5.

3.1 Verification

Table 6 shows the comparison between lightweight plastic aggregate concrete hollow circular core slab (DPHCS50-1.9 or slab 1) and lightweight crushed brick concrete hollow circular core slab specimen of Al-Azzawi and Abdul-Aziz (2018) with the same compressive strength of concrete. The slabs have (1100) length, (600 mm) width, and (120 mm) thickness and core diameter of 50 mm. Both slabs have a comparable reduction in weight which is 35%. The slabs were reinforced with bottom reinforcement only which 5 bars of (ϕ 8 mm) in short direction and 3 bars of (ϕ 8 mm) in the long direction and tested under two-line loads with shear span to effective depth ratio of ($a/d=1.9$). The table shows that the present study plastic aggregate concrete slab gives higher cracking load by 50% and higher ultimate load by 14% and lower energy absorbed by 25% or lowers ductility than the crushed brick aggregate concrete slab. Both slabs are failed with shear-flexure failure mode as shown in Fig. 3.

Table 5 Summary of samples test results

Slab No.	Abbreviation	First cracking load P_{cr} (kN)	Ultimate load P_u (kN)	$(P_{cr}/P_u) * 100\%$	Cracking deflection (mm)	Ultimate deflection (mm)	Mode of failure	Energy absorbed (kN.mm)
1	DPHCS50-1.9	70	113	62	5.50	17.7	Flexural-Shear	2623
2	NSS0-2.1	90	176.9	51	1.8	16.4	Flexural	2228
3	PSS0-2.1	90	165	54	7.0	24.9	Flexural	2817
4	NHCS75-2.1	90	180	50	2.9	24.5	Flexural	3432
5	NHCS75-1.4	125	239.4	52	3.9	18.0	Flexural-Shear	2984
6	PHCS75-2.1	90	165	54	3.4	22.07	Flexural	2805
7	PHCS75-1.4	140	246	57	4.4	24.15	Flexural-Shear	5012
8	NHCS100-2.1	65	159.3	40	2.61	39.18	Flexural-Shear	5025
9	PHCS100-2.1	95	182.1	52	3.11	18.76	Flexural	2654
10	PHSS100-2.1	90	170.7	53	2.50	20.4	Flexural	2856
11	FPHCS100-2.1	150	229	65	9.0	42.5	Flexural-Shear	7907
12	TPHCS75-2.1	85	154	55	6.7	30.58	Flexural	3529

Table 6 Verification with the previous study

Slab No.	Sample	First cracking load P_{cr} (kN)	Ultimate load P_u (kN)	$(P_{cr}/P_u) * 100\%$	Cracking deflection (mm)	Ultimate deflection (mm)	Mode of failure	Energy absorbed (kN.mm)
1	DPHCS50-1.9	70	113	62	5.50	17.7	Flexural-Shear	2623
-	AL-Azzawi and Abdul-Aziz (2018)	33	97	34	3.34	46.6	Flexural-Shear	3265

Table 7 Effect of aggregate type

Slab No.	Abbreviation	First cracking load P_{cr} (kN)	Ultimate load P_u (kN)	$(P_{cr}/P_u) * 100\%$	Cracking deflection (mm)	Ultimate deflection (mm)	Mode of failure	Energy absorbed (kN.mm)
2	NSS0-2.1	90	176.9	51	1.8	16.4	Flexural	2228
3	PSS0-2.1	90	165	54	7.0	24.9	Flexural	2817
4	NHCS75-2.1	90	180	50	2.9	24.5	Flexural	3432
6	PHCS75-2.1	90	165	54	3.4	22.07	Flexural	2805

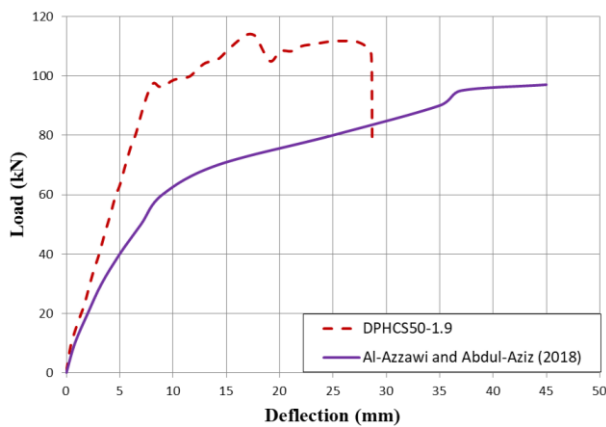


Fig. 4 Load-central deflection relationship of the present study compared with Al-Azzawi and Abdul-Aziz (2018)

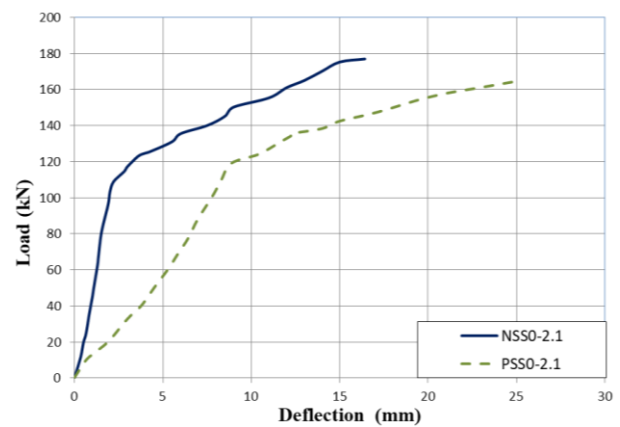


Fig. 5 Load-central deflection relationship of solid slabs with different aggregate type

The load-deflection curves are given in Fig. 4. The curves show that even both slabs are identical in all property, but the aggregate used concrete effect the behavior a lot.

3.2 Parametric study

3.2.1 Effect of aggregate type

Table 7 shows the effect of the aggregate type used in cast the samples on cracking load ultimate load and energy absorbed. The solid slab cast with natural aggregate shows higher ultimate load but lower ultimate deflection and therefore lower energy absorbed than the plastic aggregate slabs. The hollow circular core slab (core diameter 75 mm) cast with natural aggregate shows higher ultimate load ultimate deflection and therefore higher energy absorbed than the plastic aggregate slabs.

The test results reveal the importance of using PVC recycled aggregate in solid slabs as a replacement of familiar aggregate with the same shear span to effective depth ($a/d=2.1$) ratio. The PVC recycled aggregate or plastic aggregate concrete solid slabs (PSS0-2.1) gives a self-weight reduction of (21%) and reduction in ultimate capacity by 7% compared to the familiar aggregate (natural aggregate concrete solid slabs (NSS0-2.1)). The load-

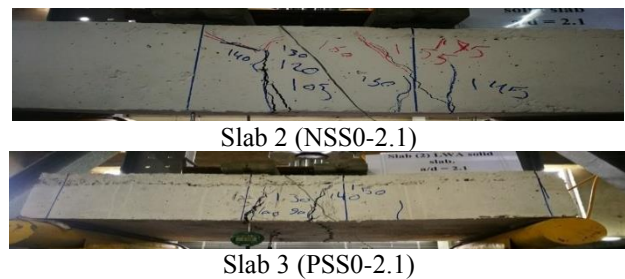


Fig. 6 Crack pattern at ultimate load for solid slabs

deflection curves improve that the behavior will be different if the aggregate type is changed in solid slab keeping all other variables constant as shown in Fig. 5.

For natural aggregate concrete solid slabs (NSS0-2.1) and plastic aggregate concrete solid slabs (PSS0-2.1), cracks are developed at about (51 and 54%) respectively of the ultimate load for a similar shear span to effective depth ($a/d=2.1$) ratio with smooth and larger crack width for the plastic aggregate concrete slab. This is maybe due to the difference in characteristics between the used natural and recycled (PVC plastic) aggregate used as shown in Fig. 6. A similar mode of failure was obtained for both slabs which are flexural failure modes.

The test results reveal the importance of using PVC

Table 7 Effect of shear span to effective depth ratio

Slab No.	Abbreviation	First cracking load P_{cr} (kN)	Ultimate load P_u (kN)	$(P_{cr}/P_u) * 100\%$	Cracking deflection (mm)	Ultimate deflection (mm)	Mode of failure	Energy absorbed (kN.mm)
4	NHCS75-2.1	90	180	50	2.9	24.5	Flexural	3432
5	NHCS75-1.4	125	239.4	52	3.9	18.0	Flexural-Shear	2984
6	PHCS75-2.1	90	165	54	3.4	22.07	Flexural	2805
7	PHCS75-1.4	140	246	57	4.4	24.15	Flexural-Shear	5012

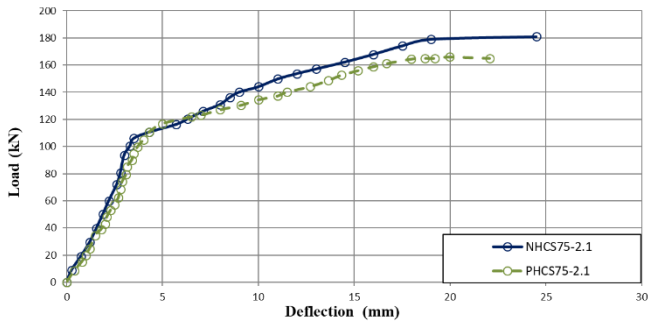


Fig. 7 Load-central deflection relationship of hollow circular core slabs with different aggregate types

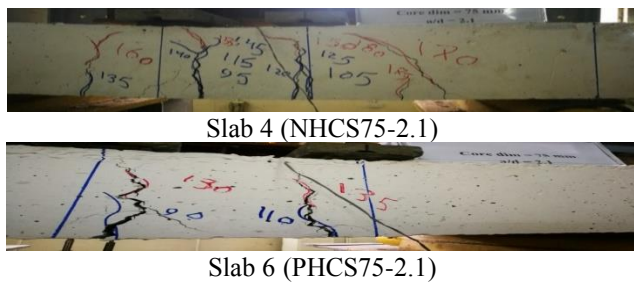


Fig. 8 Crack pattern at ultimate load for hollow core slabs

recycled aggregate in hollow circular core slab (core diameter 75 mm) as a replacement of familiar aggregate with the same shear span to effective depth ($a/d=2.1$) ratio. The PVC recycled aggregate or plastic aggregate concrete solid slabs (PHCS75-2.1) gives a self-weight reduction of 32% while the natural aggregate concrete hollow core slab (NHCS75-2.1) gives a weight reduction of 11%. The (PHCS75-2.1) slab shows a reduction in ultimate capacity by 8.3% compare to the familiar aggregate concrete slab (NHCS75-2.1). The load-deflection curves improve that the behavior will be comparable if the aggregate type is changed in hollow-core slab keeping all other variables constant as shown in Fig. 7.

For natural aggregate concrete solid slabs (NHCS75-2.1) and plastic aggregate concrete slabs (PHCS75-2.1), cracks are developed at about (50 and 54%) respectively of the ultimate load for a similar shear span to effective depth ($a/d=2.1$) ratio with smooth and larger crack width for the plastic aggregate concrete slab. This is maybe due to the difference in characteristics between the used natural and recycled (PVC plastic) aggregate used as shown in Fig. 8. A similar mode of failure was obtained for both slabs which are flexural failure modes.

Fig. 9 shows the load strain curve for the natural and plastic aggregate concrete solid slabs (same a/d) when the load increased, the plastic aggregate concrete solid slab

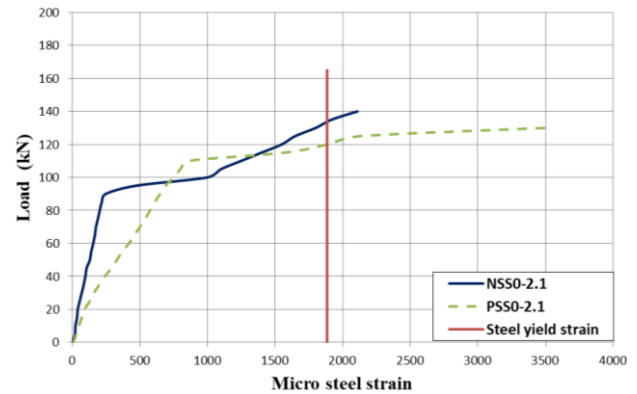


Fig. 9 Load-strain curves of solid slabs with different aggregate type

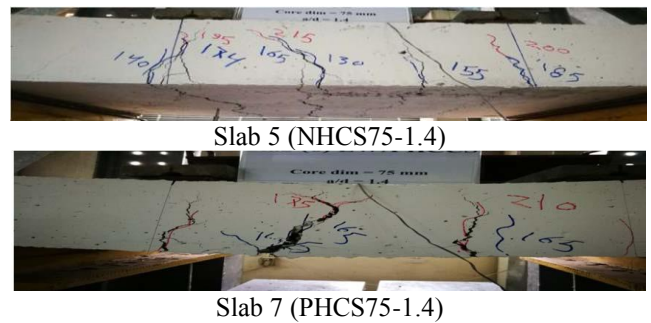


Fig. 10 Crack pattern at ultimate load for slabs 5 and 7

shows a higher recorded strain than natural aggregate and this is attributed to higher ductility behavior.

3.2.2 Effect of load location or shear span to effective depth ratio

Table 8 shows the effect of shear span to effective depth ratio (a/d) for the tested hollow circular core slabs (75 mm core diameter) on cracking load ultimate load and energy absorbed. For the natural aggregate hollow-core (NHCS75-2.1) and (NHCS75-1.4) made with core diameter (75 mm) and different a/d ratios, cracks are developed at (50-52%) from the ultimate load for a/d (2.1 and 1.4) respectively with increasing shear cracks for the 1.4 a/d ratios. The plastic aggregate hollow circular core with different a/d , (PHCS75-2.1), and (PHCS75-1.4) cracks are developed at (54-57%) respectively from the ultimate load. The difference in crack nature between slab specimens is due to a/d value. The crack patterns are shown earlier in Fig. 8 and now in Fig. 10.

The natural and plastic aggregate concrete slabs with a hollow circular core of diameter 75 mm and different ratios of a/d (2.1 and 1.4) are having a weight reduction of (11%)

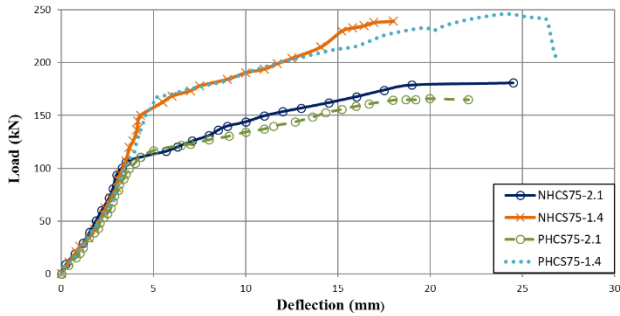


Fig. 11 Load-central deflection relationship of hollow circular core slabs with different aggregate types

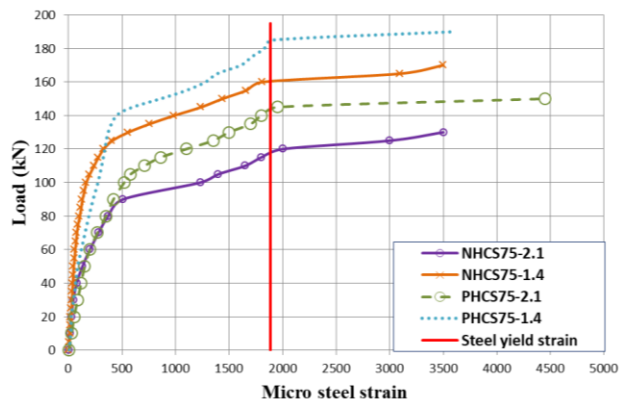


Fig. 12 Load-strain curve for slabs with different shear spans

and (32%) respectively. There is cracking and ultimate strength reduction with an increasing ratio of a/d . For a/d ratio enlarged from 1.4 to 2.1, the cracking and ultimate strength reductions were (28% and 25%) respectively for natural aggregate concrete and (36% and 33%) respectively for plastic aggregate. The load-deflection behavior shown in Fig. 11 reveals that the influence of reducing a/d will give higher loads but lower deflection for natural aggregate concrete slabs which means lower ductility.

In contrast, the influence of reducing a/d will give higher loads and deflection for plastic aggregate concrete slabs which means higher ductility. The plastic aggregate concrete slabs with ($a/d=1.4$) show the highest cracking, ultimate loads and energy absorbed compared to the other samples but the mode of failure of this slab becomes a flexural shear failure.

With increasing, the shear span or a/d ratio, the strain will be increased for both natural aggregate concrete hollow circular core slabs (slab 4 and slab 5) and plastic aggregate slabs (slab 6 and slab 7) as shown in Fig. 12.

With increasing, the shear span or a/d ratio, the strain will be increased for both natural aggregate concrete hollow

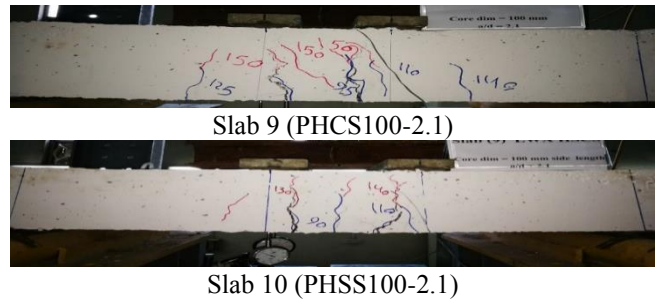


Fig. 13 Crack pattern at ultimate load for slabs 9 and 10

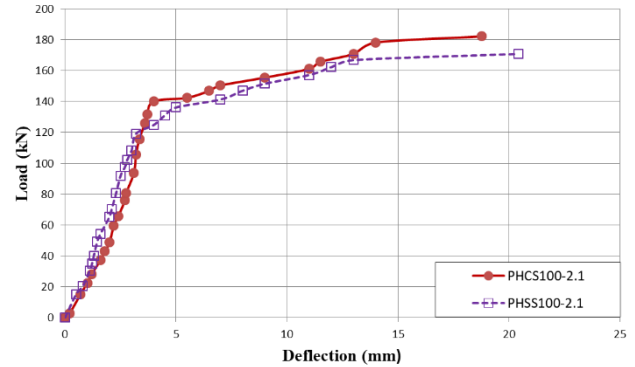


Fig. 14 Load-central deflection relationship of hollow circular and square core slabs

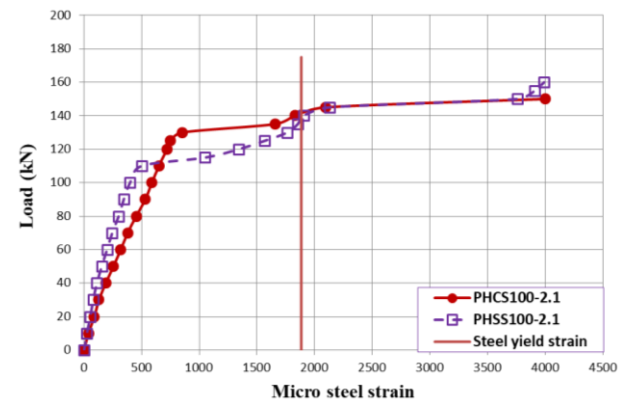


Fig. 15 Load-strain curve of hollow circular and square core slabs

circular core slabs (slab 4 and slab 5) and plastic aggregate slabs (slab 6 and slab 7) as shown in Fig. 12.

3.2.3 Effect of the core shape

Table 8 shows the effect of hollow-core shape circular or square used in tested plastic aggregate concrete slabs on cracking load ultimate load and energy absorbed. The hollow circular core slab shows higher cracking and

Table 8 Effect of the core shape

Slab No.	Abbreviation	First cracking load P_{cr} (kN)	Ultimate load P_u (kN)	$(P_{cr}/P_u) * 100\%$	Cracking deflection (mm)	Ultimate deflection (mm)	Mode of failure	Energy absorbed (kN.mm)
9	PHCS100-2.1	95	182.1	52	3.11	18.76	Flexural	2654
10	PHSS100-2.1	90	170.7	53	2.50	20.4	Flexural	2856

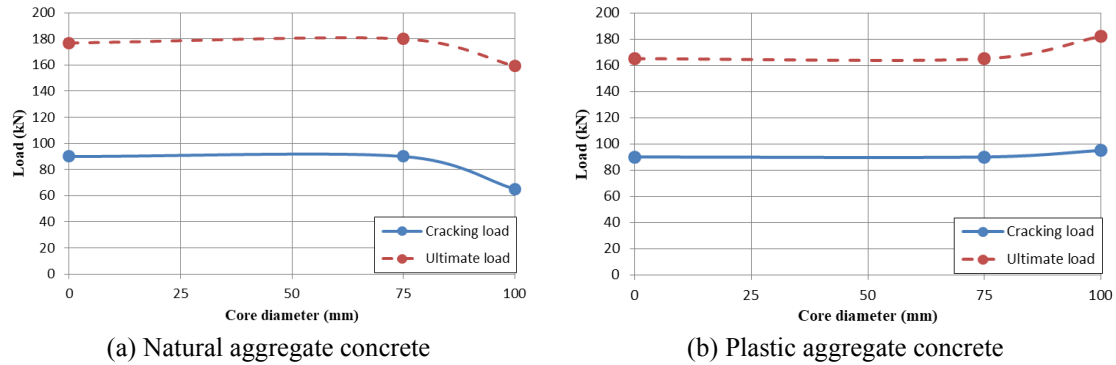


Fig. 16 Effect of core diameter on cracking and ultimate loads

Table 9 Effect of core diameter

Slab No.	Abbreviation	First cracking load P_{cr} (kN)	Ultimate load P_u (kN)	$(P_{cr}/P_u) * 100\%$	Cracking deflection (mm)	Ultimate deflection (mm)	Mode of failure	Energy absorbed (kN.mm)
2	NSS0-2.1	90	176.9	51	1.8	16.4	Flexural	2228
4	NHCS75-2.1	90	180	50	2.9	24.5	Flexural	3432
8	NHCS100-2.1	65	159.3	40	2.61	39.18	Flexural-Shear	5025
3	PSS0-2.1	90	165	54	7.0	24.9	Flexural	2817
6	PHCS75-2.1	90	165	54	3.4	22.07	Flexural	2805
9	PHCS100-2.1	95	182.1	52	3.11	18.76	Flexural	2654

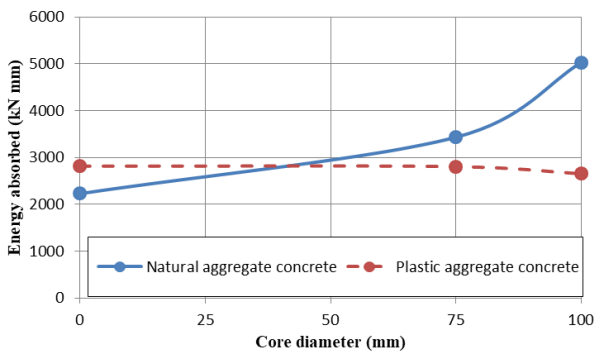


Fig. 17 Effect of core diameter on cracking and ultimate loads

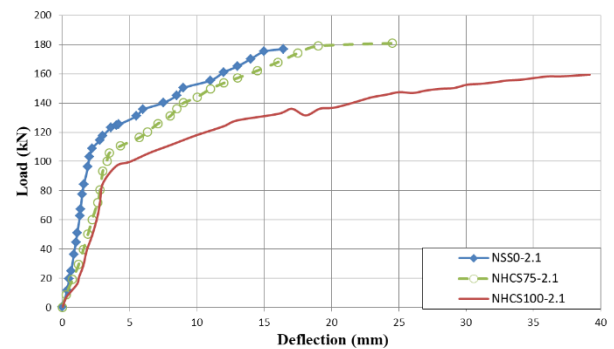


Fig. 18 Load-central deflection relationship of natural aggregate concrete slabs with different core sizes

ultimate loads but lowers ultimate deflection and therefore lower energy absorbed than the hollow square core slabs. For plastic aggregate concrete hollow circular core slab (core diameter 100 mm, $a/d=2.1$, and weight reduction 41%), or slab 9 (PHCS100-2.1), cracks are developed at (52%) from the ultimate load. At the same a/d ratio, the plastic aggregate concrete hollow square slab (core side length 100 mm, and weight reduction 46%) or slab 10 (PHSS100-2.1), cracks are developed at about (53%) of the ultimate load. Both slabs exhibit a flexural mode of failure as shown in Fig. 13.

The load-deflection behavior of slabs does not affect by the shape of the core significantly as shown in Fig. 14.

The recorded strain will be increased when the square core is used instead of the circular core at the same shear span a/d ratio as shown in Fig. 15.

3.2.4 Effect of core diameter

Table 9 shows the effect of hollow circular core

diameter used in tested concrete slabs on cracking load ultimate load and energy absorbed. For natural aggregate concrete slabs, as the core diameter increased from 0 to 100 mm, the cracking and ultimate loads are decreased by 28% and 22% respectively while the absorbed energy is increased by 25%. For plastic aggregate concrete slabs, as the core diameter increased from 0 to 100 mm, the cracking and ultimate loads are increased slightly by 5% while the absorbed energy is decreased by 5% as shown in Figs. 16 and 17. The failure modes are flexural except for the hollow circular core slab with a core diameter of 100 mm, the mode becomes flexural-shear.

The load-deflection behavior of slabs is highly affected by the size of the core as shown in Figs. 18 and 19. This is attributed to the lower stiffness in hollow-core slabs.

For the natural aggregate concrete slabs with different void sizes, the recorded steel strain is increased with increasing core diameter as shown in Fig. 20. While for plastic aggregate concrete slabs, the recorded strain is

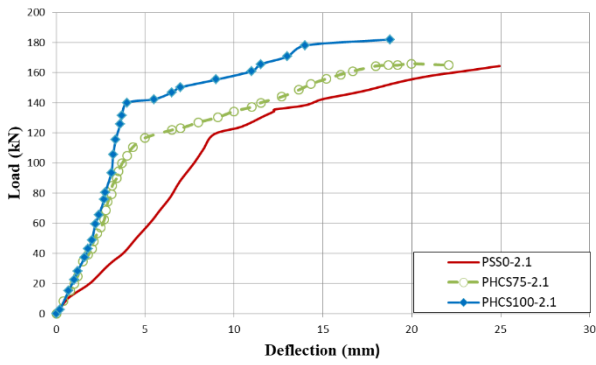


Fig. 19 Load-central deflection relationship of plastic aggregate concrete slabs with different core sizes

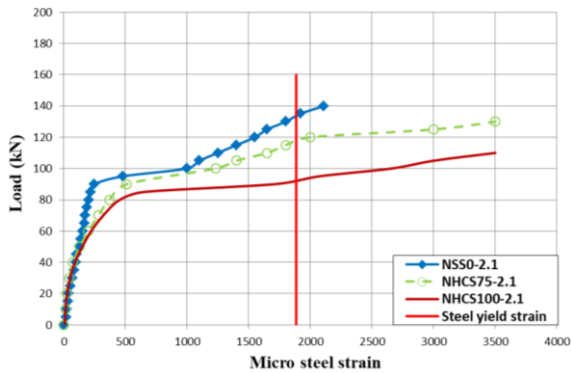


Fig. 20 Load-strain curves for natural aggregate concrete slabs with different core diameters

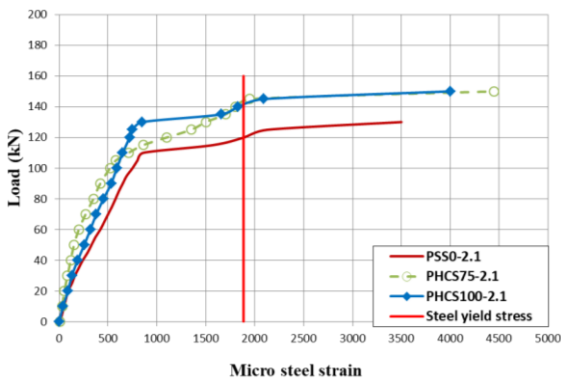


Fig. 21 Load-strain curves for plastic aggregate concrete slabs with different core diameters

decreased when core diameter increased as shown in Fig. 21.

3.2.5 Flexural reinforcement ratio

Table 10 shows the effect of flexural reinforcement ratio (ρ) of plastic aggregate concrete hollow circular core slabs

Table 10 Effect of flexural reinforcement ratio

Slab No.	Abbreviation	First cracking load P_{cr} (kN)	Ultimate load P_u (kN)	P_{cr}/P_u *100 %	Cracking deflection (mm)	Ultimate deflection (mm)	Mode of failure	Energy absorbed (kN.mm)
9	PHCS100-2.1	95	182.1	52	3.11	18.76	Flexural	2654
11	FPHCS100-2.1	150	229	65	9.0	42.5	Flexural-Shear	7907



Slab 9 (PHCS100-2.1)



Slab 11 (FPHCS100-2.1)

Fig. 22 Crack pattern at ultimate load for hollow core slabs with different steel ratio

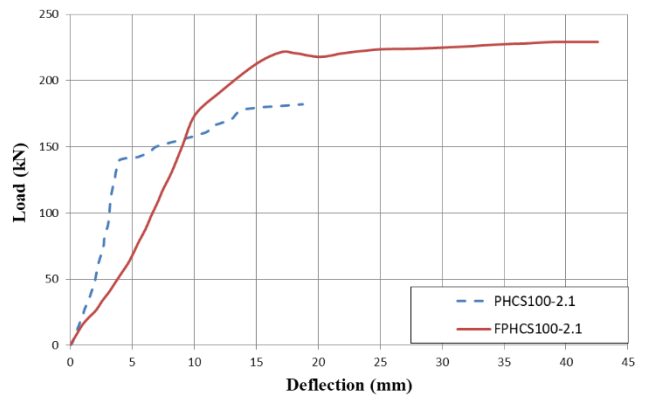


Fig. 23 Load-deflection relationship for plastic aggregate concrete hollow circular core slabs with different reinforcement ratio $\rho=0.002$ and $\rho=0.004$

(core diameter 100 mm and $1/d$ 2.1) on cracking load, ultimate load, and energy absorbed. As the reinforcement ratio increased from (0.002 or 0.004), the cracking load, ultimate load, and absorbed energy are increased by 58%, 26%, and 200% respectively. As the resisting moment increased for steel ratio (0.004), the mode of failure changed from flexure to flexure-shear. The crack pattern shown in Fig. 22 reveals this behavior.

The load-deflection curves show similar behaviors as shown in Fig. 23. The lower steel ratio slab has a higher stiffness at the beginning of the loading stage after that the higher steel ratio slabs exhibit the higher stiffness.

Slab with higher reinforcement amount show (at same load level) lesser strains as shown in Fig. 24.

3.2.6 Slab thickness

Table 11 shows the effect of slab thickness of plastic aggregate concrete hollow circular core slabs (core diameter 75 mm and $1/d$ 2.1) on cracking load, ultimate load, and energy absorbed. As the thickness decreases 200 to 175, the cracking and ultimate loads are decreased by 5% while the

Table 11 Effect of slab thickness

Slab No.	Abbreviation	First cracking load P_{cr} (kN)	Ultimate load P_u (kN)	$(P_{cr}/P_u) * 100\%$	Cracking deflection (mm)	Ultimate deflection (mm)	Mode of failure	Energy absorbed (kN.mm)
6	PHCS75-2.1	90	165	54	3.4	22.07	Flexural	2805
14	TPHCS75-2.1	85	154	55	6.7	30.58	Flexural	3529

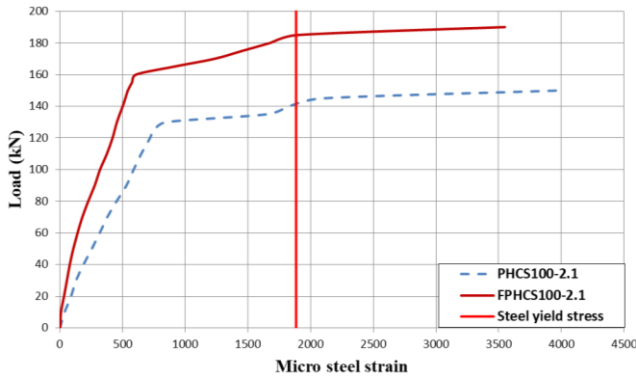


Fig. 24 Load-strain curves for slabs with different steel ratio

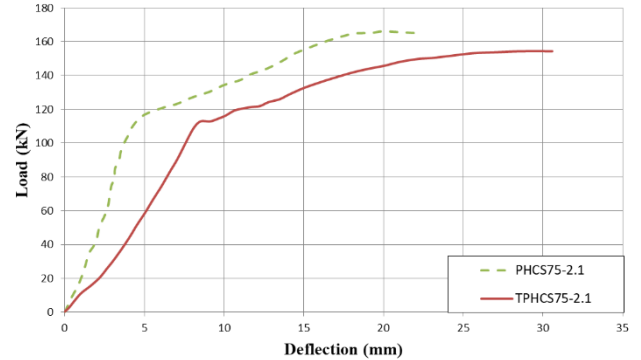


Fig. 26 Load-deflection relationship of hollow cores slabs with different thicknesses

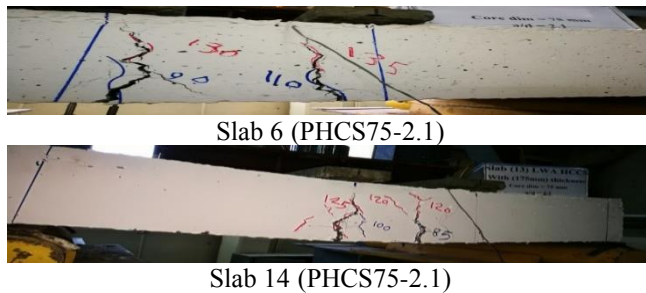


Fig. 25 Crack pattern at ultimate load for hollow core slab with different thicknesses

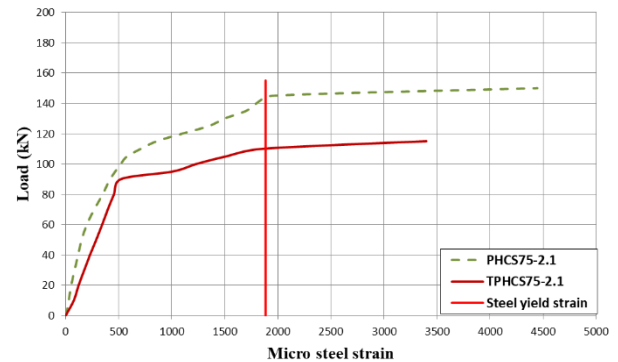


Fig. 27 Load-strain curves for hollow core slabs with different thicknesses

absorbed energy is increased by 26%. The mode of failure is not affected by slab thickness as shown in Fig. 25. The cracking deflection and ultimate deflection decreased with increasing slab thickness.

Similar trends for the load-deflection curves were obtained for the different slab thicknesses as shown in Fig. 26. The stiffness of the slab increased with increasing thickness.

From curves in Fig. 27, at the same level of load, with enlargement thickness of the slab, the strain will be decreased due to decreasing the curvature of the slab.

5. Conclusions

The following conclusions can be drawn based on the investigation results of the experimental work.

- Slabs reduction in weight can be carried out by using two types. The first by using the waste of PVC plastic as recycled coarse aggregate and the second is by utilizing the hollow core. In this research, the maximum weight reduction due to using recycled aggregate (PVC) was (21%) and due to using hollow section was (25.0%). The total reduction was (46%). Sustainable concrete can be obtained using PVC plastic waste, which is utilized as a recycled coarse aggregate for producing structural

recycled concrete with a strength of compressive at about 28.0 MPa.

- The comparison between the present study lightweight plastic aggregate concrete hollow circular core slab and the lightweight crushed brick concrete hollow circular core slab specimen from the previous study revealed that the present study plastic aggregate concrete slab gives higher cracking load by 50% and higher ultimate load by 14% and lower energy absorbed by 25% or lowers ductility than the crushed brick aggregate concrete slab. Both slabs are failed with shear-flexure failure mode.

- The results revealed that the solid slab cast with natural aggregate shows higher ultimate load but lower ultimate deflection and therefore lower energy absorbed than the plastic aggregate slabs. The hollow circular core slab (core diameter 75 mm) cast with natural aggregate shows higher ultimate load ultimate deflection and therefore higher energy absorbed than the plastic aggregate slabs. For natural and plastic aggregate concrete solid slabs, cracks are developed at about (50 and 54%) respectively of the ultimate load for a similar shear span to effective depth ($a/d=2.1$) ratio with smooth

and larger crack width for the plastic aggregate concrete slab.

- The natural and plastic aggregate concrete slabs with hollow circular core show cracking and ultimate strength reduction with an increasing ratio of a/d . For a/d ratio enlarged from 1.4 to 2.1, the cracking and ultimate strength reductions were (28% and 25%) respectively for natural aggregate concrete and (36% and 33%) respectively for plastic aggregate. The load-deflection behavior reveals that the influence of reducing a/d will give higher loads but lower deflection for natural aggregate concrete slabs which means lower ductility. In contrast, the influence of reducing a/d will give higher loads and deflection for plastic aggregate concrete slabs which means higher ductility. The plastic aggregate concrete slabs with ($a/d=1.4$) show the highest cracking, ultimate loads and energy absorbed compared to the other samples but the mode of failure of this slab becomes a flexural shear failure.
- For natural aggregate, the entity of voids in the one-way slabs minimizes their cracking and ultimate capacities. While for PVC RA concrete, hollow cores will cause an increase in cracking and ultimate capacities in values relied on the dimension and voids form.
- The change in the shape of the core from circular to square and the use of (100 mm) side length led to reducing the weight by about (46%). The cracking and ultimate strength is reduced by about (5%-6%) respectively. With similar values of deflection. The mode of failure will remain flexural.
- An increase in cracking and ultimate strength by about (58% and 26%) respectively with increasing reinforcement amount from (5bars $\phi 8$ mm) to (8bars $\phi 8$ mm) but the mode of failure will be changed to shear-flexural.
- If the thickness of the slab changed from (200 mm to 175 mm) the result shows the reduction of cracking and ultimate strength by about (6%-7%) respectively.

References

- Abramski, M., Albert, A., Nitsch, A. and Schnell, J. (2010), "Bearing behavior of biaxial hollow core slabs", *34th International Symposium on Bridge and Structural Engineering*, Venice, January.
- ACI 211.1 (1991), Standard Practice for Selecting Proportions for Normal, Heavyweight and Mass Concrete, American Concrete Institute, 6-38.
- ACI 213R-03 (2003), Guide for Structural Lightweight-Aggregate Concrete, American Concrete Institute, Detroit, U.S.A.
- ACI318-14, (2014), Building Code Requirements for Structural Concrete and Commentary, American Concrete Institute, Detroit, U.S.A.
- Al-Azzawi, A.A. and Abdul Al-Aziz, B.A. (2018), "Behavior of reinforced lightweight aggregate concrete hollow core slabs", *Comput. Concrete*, **21**(2), 117-126. <https://doi.org/10.12989/cac.2018.21.2.117>.
- Al-Azzawi, A.A. and Abed, S.A. (2017), "Investigation of the behavior of reinforced concrete hollow-core thick slabs", *Comput. Concrete*, **19**(5), 567-577. <https://doi.org/10.12989/cac.2017.19.5.567>.
- Al-Azzawi, A.A. and Al-Asdi, A.J. (2017), "Behavior of one way reinforced concrete slabs with styropor blocks", *Adv. Concrete Constr.*, **5**(5), 451-468. <http://dx.doi.org/10.12989/acc.2017.5.5.451>.
- Al-Azzawi, A.A. and Al-Azzawi, A.A. (2020), "Mechanical properties of green concrete", *IOP Conf. Ser.: Mater. Sci. Eng.*, **888**(1), 012022. <https://doi.org/10.1088/1757-899X/888/1/012022>.
- Al-Azzawi, A.A., Daud, R.A. and Daud, S.A. (2020), "Behavior of tension lap spliced sustainable concrete flexural members", *Adv. Concrete Constr.*, **9**(1), 83-92. <https://doi.org/10.12989/acc.2020.9.1.083>.
- Alamgir, M. and Ahsan, A. (2007), "Municipal solid waste and recovery potential: Bangladesh perspective", *Iran. J. Environ. Hlth. Sci. Eng.*, **4**(2), 67-76.
- ASTM C 1240 (2005), Standard Specification for Silica Fume Used in Cementitious Mixtures, American Society for Testing and Material.
- Brunesi, E., Bolognini, D. and Nascimbene, R. (2014), "Evaluation of the shear of precast-prestressed hollow core slab: numerical and experimental comparison", *Mater. Struct.*, **48**(5), 1503-1521. <https://doi.org/10.1617/s11527-014-0250-6>.
- Daud, R.A., Cunningham, L.S. and Wang, Y.C. (2015), "Static and fatigue behaviour of the bond interface between concrete and externally bonded CFRP in single shear", *Eng. Struct.*, **97**, 54-67. <https://doi.org/10.1016/j.engstruct.2015.03.068>.
- Daud, S.A., Forth, J.P. and Nikitas, N. (2018), "Time-dependent behaviour of cracked, partially bonded reinforced concrete beams under repeated and sustained loads", *Eng. Struct.*, **163**, 267-280. <https://doi.org/10.1016/j.engstruct.2018.02.054>.
- de Brito, J. and Saikia, N. (2013), *Recycled Aggregate in Concrete*, Springer-Verlag, London.
- Haruna, S.I. (2014), "Flexural behavior of precast pre-stressed concrete hollow core slabs with cast-in-place concrete topping", Master's Thesis, Civil Engineering, Atılım University.
- Iraqi Specification No. 45 (1984), Aggregate from Natural Sources for Concrete, Central Agency for Standardization and Quality Control, Planning Council, Baghdad, Iraq.
- Iraqi Specification No.5 (1984), Portland Cement, Central Agency for Standardization and Quality Control, Planning Council, Baghdad, Iraq.
- Khalid, F.S., Irwan, J.M., Ibrahim, M.H.W., Othman, N. and Shahidan, S. (2018), "Performance of plastic wastes in fiber-reinforced concrete beams", *Constr. Build. Mater.*, **183**, 451-464. <https://doi.org/10.1016/j.conbuildmat.2018.06.122>.
- Khatib, J., Jahami, A., Elkordi, A. and Baalbaki, O. (2019), "Structural performance of reinforced concrete beams containing plastic waste caps", *Mag. Civil Eng.*, **91**(7), 73-79. <https://doi.org/10.18720/MCE.91.7>.
- Lee, D.H., Park, M., Oh, J., Kim, K.S., Im, J. and Seo, S. (2014), "Web-shear capacity of prestressed hollow core slab unit with consideration on the minimum shear reinforcement requirement", *Comput. Concrete*, **14**(3), 211-231. <https://doi.org/10.12989/cac.2014.14.3.211>.
- Mohammed, A.A. (2017), "Flexural behavior and analysis of reinforced concrete beams made of recycled PET waste concrete", *Constr. Build. Mater.*, **155**, 593-604. <https://doi.org/10.1016/j.conbuildmat.2017.08.096>.
- Rahman, M.K., Baluch, M.H., Said, M.K. and Shazali, M.A. (2012), "Flexural and shear strength of pre-stressed precast hollow-core slabs", *Arab. J. Sci. Eng.*, **37**(2), 443-455.
- Said, M.K., Rahman, M.K. and Baluch, M.K. (2012), "Analysis and design of prestressed precast hollow core slabs using strut and tie method", *Arab. J. Sci. Eng.*, **37**, 457-468.
- Stephen, C. (2013), "Hollow core manufacturing and factory design", *Ind. Concrete J.*, 20-25.
- Wariyatno, N.G., Haryanto, Y. and Sudiboyo, G.H. (2017),

- “Flexural behavior of precast hollow core slab using PVC pipe and Styrofoam with different reinforcement”, *Procedia Eng.*, **171**, 909-916. <https://doi.org/10.1016/j.proeng.2017.01.388>.
- Yang, X., Yao, Y., Chu, Y. and Yang, T. (2014), “Study on the calculation method for flexural capacity of pre-stressed concrete hollow-core slabs strengthened with CFRP”, *Appl. Mech. Mater.*, **578-579**, 1366-1369. <https://doi.org/10.4028/www.scientific.net/AMM.578-579.1366>.

JK